

Optimizing 3D Crack Front Shapes by a Predictor-Corrector Scheme for 3D Mixed-Mode Problems

K. Kolk and G. Kuhn

Institute of Applied Mechanics, University of Erlangen-Nuremberg,
Egerlandstr. 5, 91058 Erlangen, Germany
e-mail: kolk@ltm.uni-erlangen.de, gkuhn@ltm.uni-erlangen.de

ABSTRACT. *A predictor-corrector scheme capable of mixed-mode problems is presented to optimize the shape of 3D crack fronts within the 3D simulation of fatigue crack growth. It enables one to follow and/or predict crack paths as realistic as possible. The whole procedure is embedded in an automatic incremental crack growth algorithm for arbitrary three-dimensional problems with linear-elastic material behavior. The numerical simulation is based on the 3D dual boundary element method (Dual BEM) and on the optimized evaluation of very accurate stress intensity factors (SIFs) and T-stresses. As part of the proposed predictor-corrector scheme, 3D singularities along the crack front especially in the vicinity of the intersection of the crack front and the boundary are considered. The knowledge about these singularities allows the specification of crack front shapes with bounded energy release rate. Additionally, it is assumed that the crack front shape ensures a constant energy release rate along the whole crack front. A numerical example with a complex cross section is presented to show the efficiency of the proposed crack growth criterion. A comparison to recent experimental results shows good agreement.*

INTRODUCTION

In fracture mechanics analyses one has to distinguish between monotonically increasing and cyclic loading conditions. The more important case is the cyclic one, because much lower loads lead to crack growth, which can be divided into three stages (retardation, stable fatigue crack growth and the transition to unstable crack growth).

The stage of stable crack growth is investigated in terms of linear-elastic fracture mechanics. The aim is to describe this stage as realistic as possible. Then, a reliable validation of real or hypothetical cracks is feasible. In the present paper it is assumed, that a threshold value concerning the crack growth is always exceeded along the whole crack front leading to a completely growing crack. The opposite case, that this threshold value is only locally exceeded at a crack front, is experimentally investigated in [1].

As the crack growth is a non-linear process, an incremental procedure is required. It includes the three steps: a) the analysis of the state of stresses and strains, b) the

determination of the new crack geometry and c) the update of the numerical model for the next increment.

The stress analysis is performed with the 3D Dual BEM. The determination of the new crack geometry is based on an appropriate 3D crack growth criterion. A predictor-corrector scheme based on the energy release rate, respectively the SIFs, is proposed to optimize the crack front shape and its position. This scheme can be applied to general 3D specimens under arbitrary loading conditions. The most important case is mode-I, as such conditions are often the reason for failure in industrial applications. An example regarding this mode will be presented to show the efficiency of the proposed predictor-corrector scheme. Furthermore, the application of the proposed scheme to mixed-mode problems will be discussed.

STRESS ANALYSIS

The boundary value problem as shown in Fig. 1 is solved by the 3D dual boundary element method (3D Dual BEM) [2].

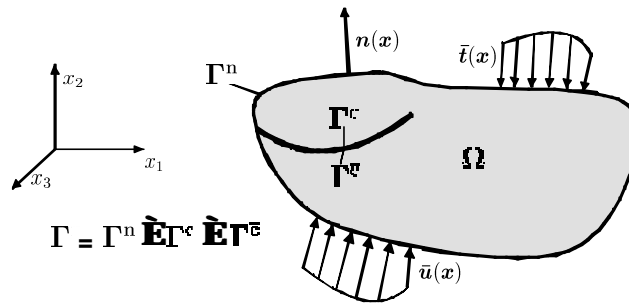


Figure 1. Sketch of the boundary value problem.

The cracked body $\Omega \in \mathbf{R}^3$ is homogeneous and isotropic with linear elastic material behavior. Ω is bounded by the normal boundary Γ^n and the coincident crack surfaces Γ^c and $\bar{\Gamma}^c$. Dirichlet and Neumann boundary conditions are applied along the boundary Γ . The relevant displacement boundary integral equations (BIE) are evaluated in the framework of a collocation method on Γ^n and only on one crack surface. Otherwise a singular system matrix would occur [3]. To avoid this, the coincident crack surfaces need to be separated. In the present context, dual integral formulations are used [4]. Hence, the hypersingular traction BIE is additionally evaluated on the remaining crack surface.

It is a special advantage of the 3D Dual BEM for the simulation of 3D crack growth, that this procedure can be used within a single sub region. Especially in the area of high stress concentrations - ahead of the crack front - no discretization is needed.

Arbitrarily shaped 3D cracks under general load conditions can be analyzed. The procedure is robust and leads to very accurate results. However, the simulation of propagating cracks is costly, because a lot of increments are necessary to follow a crack

path. The most time consuming step is the solution of the boundary value problem with the 3D Dual BEM, which has to be performed in each increment. Within the stress analysis the solution of the linear algebraic system of equations plays the dominant role. The application of the DDM (Dual Discontinuity Method) [2] eliminates one crack surface with respect to the integration and leads to a smaller system of equations, which has to be solved.

As long as the system of linear equations fits into random access memory (RAM), the iterative GMRES solver is used. It accelerates the stress analysis compared to a direct solver significantly. If there are only slight changes in the new crack front shape, the solution of the last increment can be chosen as the start solution of the new increment. It results in an additional speed-up of approximately 30%.

But if the system of linear equations no longer fits into RAM, additional effort is required to still be able to use the fast iterative solver. In this case, the so-called multipole expansion method (MEM) [5,6] can be applied, as it becomes advantageous when exceeding a certain number of degrees of freedom.

AUTOMATIC 3D CRACK GROWTH ALGORITHM

The 3D crack growth algorithm consists of three steps, which are shown in Fig. 2.

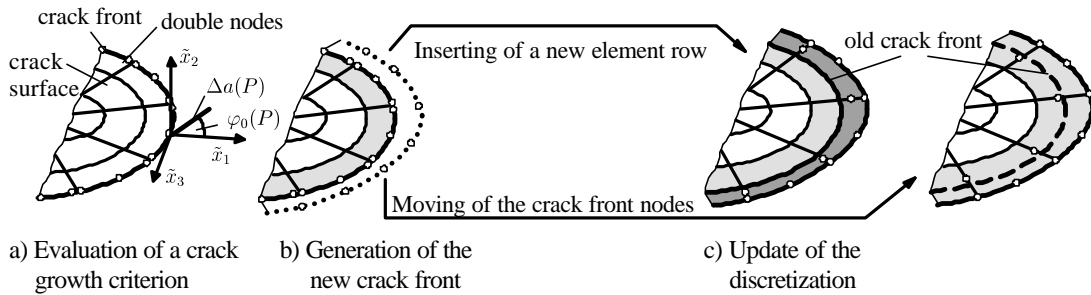


Figure 2. Basics of the crack growth algorithm.

First of all, fracture mechanics parameters are evaluated along the whole crack front. The SIFs and additionally the T-stresses are calculated from the numerical stresses in the crack near-field very accurately via an optimized local extrapolation method based on a regression analysis controlled by the minimization of the standard deviation [7]. The asymptotic distribution of these stresses related to a cartesian crack front coordinate system with an associated polar coordinate system in the $(\tilde{x}_1, \tilde{x}_2)$ -plane, cf. Fig. 2a, is given by:

$$\mathbf{s}_{ij}(r, \mathbf{j}, P) = \sum_{M=1}^{\text{III}} \frac{K_M(P)}{\sqrt{2pr}} f_{ij}^M(\mathbf{j}) + T_{ij} + O(r) \quad (1)$$

for a point P on a smooth crack front [8]. The intensity of the typical square-root singularity is characterized by the SIFs K_M ($M = \text{I,II,III}$). $f_{ij}^M(\mathbf{j})$ denote the corresponding angular functions while T_{ij} denote the T-stresses.

For every crack front node a new position is determined by the evaluation of a suitable crack growth criterion. It includes the determination of the kink angle and the crack extension. With these two quantities the shape and position of the new crack front can be defined.

Next, the gap between the old and new crack front can be closed during the update of the numerical model via two options. If there are only small local crack extensions (*corrector steps*), the old crack front nodes are moved towards the new crack front. In case of significant crack extensions along the whole crack front (*predictor steps*) a new row of elements can be inserted as shown in Fig. 2c.

Special attention is needed in case of surface breaking cracks, as two important aspects have to be considered. Firstly, the normal boundary Γ^n has to be taken into account during the update of the discretization. Ensuring an optimized mesh an automatic local re-meshing procedure is applied. Secondly, due to the possible change of singularities in the vicinity of the intersection of the crack front and the free surface, a 3D singularity analysis is necessary.

Finally, the numerical model for the next increment is generated in a fully automatic way.

3D CORNER SINGULARITIES

The classical SIFs are linked to the square-root singularity. But this kind of singularity generally doesn't hold for non-smooth parts of the crack front, especially in the vicinity of the intersection of the crack front with the boundary in case of surface breaking cracks. At such points one has to consider 3D corner singularities. The knowledge of the present singularities along the crack front is one of the basic parts of the proposed predictor-corrector scheme.

Around the singular point O with coordinates $\mathbf{x}_0 \in \Omega \subset R^3$, an \mathbf{e} -neighborhood $\Omega^{\mathbf{e}}$ is considered. The corresponding elastic solution in the vicinity of the singular point O related to a spherical coordinate system, which is centered in O, is asymptotically expanded in the form

$$u_i(\mathbf{r}, \mathbf{q}, \mathbf{j}, \mathbf{O}) = \sum_{L=1}^{\infty} K_L^*(\mathbf{O}) \mathbf{r}^{\mathbf{a}_L} g_i^L(\mathbf{q}, \mathbf{j}, \mathbf{O}). \quad (2)$$

\mathbf{a}_L denote the asymptotic exponents satisfying $\mathbf{a}_L > -0.5$ from the elastic energy point of view, cf. [9], and g_i^L are the corresponding angular functions. The asymptotic exponents are now linked to generalized intensity factors K_L^* . The vicinity $\Omega^{\mathbf{e}}$ around O is given by $\Omega^{\mathbf{e}} := \Omega \cap \Omega^{\mathbf{e}}$ and $\Omega^{\mathbf{e}} := \{\mathbf{x} \in \mathbf{R}^3 : |\mathbf{x} - \mathbf{x}_0| < \mathbf{e}\}$.

The solution of a quadratic eigenvalue problem in terms of α with the associated eigenvectors g_i provides the asymptotical exponents α_L [9].

The interval $-0.5 < \mathbf{a}_L < 1$ is considered, because the asymptotic behavior is focused whereas the rigid body motion modes are excluded as they are known. \mathbf{a}_L depends on the geometrical situation around the singular point as well as on material parameters. For homogenous and isotropic materials it only depends on the Poisson's ratio ν .

For $\mathbf{a}_L = 0.5$ the intensity factor K_L^* may correspond with one of the classical stress intensity factors K_M . In general, one cannot distinguish between mode-I,II,III any more but only between symmetric and antisymmetric modes. The symmetric mode corresponds to mode-I and the antisymmetric modes can be either pure mode-II or pure mode-III or a combination of both.

Though, \mathbf{a}_L is only different from 0.5 at some special points and if the classical SIF-concept is used to describe the behavior in the crack-near field, there are two options. Firstly, a general intensity factor concept can be designed. Secondly, the classical SIF-concept is kept and the SIFs at these special points are defined in an asymptotical sense [10]. Following Eq. 2 gives $u \sim O(\mathbf{r}^{\alpha_L})$ and therefore $\mathbf{s} \sim O(\mathbf{r}^{\alpha_L-1})$. This means, if \mathbf{a}_L is greater than 0.5, K_M tends to zero and for $\mathbf{a}_L < 0.5$ the classical SIF K_M tends to infinity.

Hence, the exponents \mathbf{a}_L have to be known to determine the classical SIFs asymptotically. But this is not the only application of these 3D singularities as shown in [11]. Moreover, crack front elements incorporating the relevant singular exponents can be designed to improve corresponding numerical calculations. Concerning the simulation of crack propagation, it is advantageous that the angle between the crack front and the free surface can be determined by the assumption of $\mathbf{a}_L = 0.5$. A first agreement of this relationship in case of mode-I can be found in [11]. Detailed experimental investigations regarding different cross sections and crack front shapes yielding the same correlation are presented in [1]. In case of mixed-mode problems the crack front angle should be adjusted in a way that the smallest asymptotical exponent tends to 0.5. This results in a crack front shape with a bounded energy release rate. The coincidence to experimental findings including observed crack front angles is shown in [12].

As the crack front angle can be determined by a singularity analysis for a given crack configuration, it is possible to modify the geometry to get a predefined angle. This effect is reported in [11], where the class of square-root singularity specimens is proposed.

PREDICTOR-CORRECTOR SCHEME

The position of the new crack front during fatigue crack growth is essentially influenced by two parameters; the crack extension and the kink angle. So far, both parameters are determined by a predictor procedure, as discussed in the next subsection. Afterwards, all proposed corrector steps will be presented. This results in a predictor-corrector scheme concerning the crack extension with an implicit correction of the kink angle.

Predictor

For the determination of the crack extension $\Delta a(P)$ at a crack front point P, a user-defined incremental length Δa_0 is specified. This length is distributed along the crack front depending on an appropriate fracture mechanics parameter (an effective SIF or the energy release rate). The maximum crack extension is either assigned to a maximum or an average value of these parameters and is distributed linearly along the crack front. Alternatively, an exponential distribution based on the Paris Law is applied. But the shape of the crack front and therefore the resulting crack path depends on the amount of Δa_0 . Thus, corrector steps are introduced to improve the shape of the crack front.

The kink angle $\mathbf{j}(P)$ is determined by the maximum tangential stress (MTS)-criterion. This criterion provides the angle of a differential crack extension depending only on K_I and K_{II} . Thus, the SIF K_{III} is missing and only the tangent to a possibly deflecting crack path is described. As the crack deflection is not included a “zigzag” path around the smooth curved path may occur. Furthermore the crack extension is finite in the incremental crack growth procedure and not differential for which the angle holds. The missing SIF can be additionally included following the proposition in [13], that the crack growth angle is perpendicular to the maximum principle stress on an imaginary cylindrical sphere around the crack front. Including the SIF K_{III} for the determination of the crack deflection implicates actually an additional angle around the \tilde{x}_1 -axis. This angle corresponds to the mostly typical phenomenon of the formation of facets if mode-III is present. But this behavior is not considered, as it is not modeled yet. The consideration of K_{III} improves the kink angle but there is still a tangent described.

Corrector

Starting with mode-I conditions, the corrector steps can easily be explained. There is a close relationship between the crack front shape and a corresponding fracture mechanics parameter, e.g. K_I . Based on preliminary tests, it is assumed and mostly verified that K_I controls the crack growth and the crack front will propagate in a way that K_I is constant along the whole crack front. For the determination of K_I it is essential that the square-root singularity holds along the crack front, even at both ends in case of surface breaking cracks. Knowing the present value of the asymptotic exponent α_L one has to adjust the angle \mathbf{g} between the tangent of the crack front and the negative normal vector of the free surface to satisfy the square-root singularity. The crack extension is performed on basis of the energy release rate, because it has the mostly physical meaning, with the following distribution

$$\Delta a(P) = \Delta a_0 \frac{G(P) - C \cdot G_{\min}}{G_{\max}}. \quad (3)$$

The corrector C is equal to one if a corrector step and equal to zero if a predictor step is performed. Within an iterative procedure the practical constance of K_I is ensured. The crack front will be locally corrected in the direction of the crack growth relatively to the minimum of G . This procedure can be named iterative forward predictor-corrector

scheme. The crack grows according to the maximum energy release rate while minimizing the amount of newly generated crack surfaces.

The condition of a constant K_I is equivalent to the constance of G for mode-I and no longer sufficient for mixed-mode. In this case, constance is only claimed for G , which leads to the extension of the predictor-corrector scheme to mixed-mode problems. Additionally, it is also no longer sufficient to consider only one relevant singularity at the crack front intersections. Up to four different exponents may occur and it is a reasonable choice to use the smallest one to adjust the crack front angle ensuring a crack front with a bounded energy release rate.

The correction of the kink angle is implicitly performed by considering the T-stresses in the calculation of the kink angle, cf. [14]. Then, this angle additionally depends on the Poisson's ratio and the crack extension. As the crack extension is distributed according Eq. 3, the kink angle is automatically corrected following the crack deflection closely.

NUMERICAL EXAMPLE

A fatigue crack growth experiment is shown to demonstrate the efficiency of the proposed predictor-corrector scheme. This scheme was introduced for mixed-mode problems, but only mode-I will be considered. On one hand, a lot of failures in industrial applications are caused by this mode. On the other hand, recent well documented experimental results by M. Heyder are available for a 4-point bending specimen with a complex "triple"-T-shaped cross section as shown in Fig. 3.

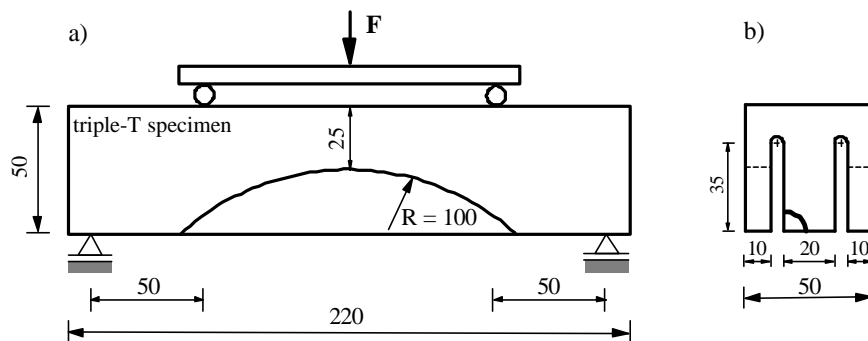


Figure 3. a) 4-point bending specimen; b) "triple"-T cross section.

A quasi-elliptical corner crack is located in the center leg in half of the length of the specimen. The maximum force of the cyclic load was $F = 3\text{kN}$. The transparent material PMMA ($E \approx 3.6\text{ GPa}$, $\nu = 0.36$) was used to be able to document the growing crack fronts. Starting from the initial crack front the load was subsequently decreased to $F = 1.6\text{kN}$ ensuring stable crack growth conditions along the whole crack front. When the crack approaches the rear surface, unstable crack growth occurs but the crack grows rapidly only a few millimeters. Afterwards, stable crack growth could be monitored once again.

Firstly, the corner singularities at both ends of the crack front should be considered. In both cases the crack surface is perpendicular to the free surface. Ensuring a valid square-

root singularity along the whole crack front, which is assumed in the crack growth criterion, the crack front angle is enforced. A reliable singularity analysis yields $g = 13.845^\circ$. As there will be no further change of the geometrical situation at both ends of the crack front during mode-I crack growth, the specified angle will not change either.

Figure 4a underlines the need of corrector steps as the predictor scheme leads to a crack path that grows slower at the bottom and faster at the left side relatively to the experimental results.

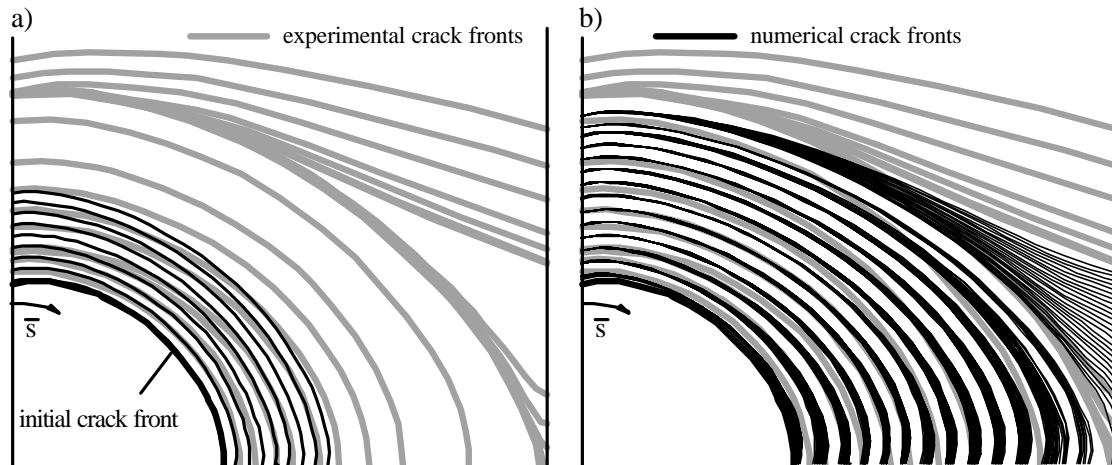


Figure 4. Comparison of experimental and numerical crack front shapes in case of the a) predictor and b) predictor-corrector procedure.

In contrast, a very good agreement can be observed when applying corrector steps, cf. Fig. 4b. It can be seen, that the crack stops growing at the left side even if the threshold value is exceeded at this point while on the right hand side unstable crack growth occurs. The agreement of the simulated crack front shapes to the experimental ones at the end of the unstable phase is also remarkable.

REFERENCES

1. Heyder, M., Kuhn, G. (2003) to be presented at *Int. Conference FCP 2003*.
2. Partheymüller, P., Haas, M., Kuhn, G. (2000) *Engng. Anal. Boundary Elements* **24**, 777-788.
3. Cruse, T.A. (1972) In: *The surface crack: physical problems and computational solutions*, pp.153-170, Swedlow, J.L. (Ed.), ASME.
4. Portella, A., Aliabadi, M.H., Rooke, D.P. (1992) *Int. J. Num. Meth. Engng* **33**, 1269-1287.
5. Popov, V., Power, H. (2001) *Engng Anal. Boundary Elements* **25**, 7-18.
6. Kolk, K., Kuhn, G. (2003) In: *Proc. 2nd MIT Conf. on Computational Fluid and Solid Mechanics*, accepted, Bathe, K.J. (Ed), Elsevier, Netherlands.
7. Kolk, K., Kuhn, G. (2001) In: *Proc. of the 2nd European Conference on Computational Mechanics*, CD, Waszczyszyn, Z., Pamin, J. (Eds), ECCM, Cracow.
8. Leblond, J., Torlai, O. (1992) *Int. J. Elasticity* **29**, 97-131.

9. Dimitrov, A., Andrä, H., Schack, E. (2001) *Int. J. Meth. Engng* **52**, 805-827.
10. Nakamura, T., Parks, D.M. (1989) *Int. J. Solids Structures* **25**, 1411-1420.
11. Kolk, K., Mishuris, G., Kuhn, G. (2003) In: *IUTAM Symp. on Asymptotics, Singularities and Homogenisation Problems in Mech.*, in press, Movchan, A.B. (Ed.), Kluwer, Netherlands.
12. Dimitrov, A., Buchholz, F.G., Schnack, E. (2002) In: *Proc. of the 5th World Congress on Comp. Mech.*, <http://wccm.tuwien.ac.at>, Mang, H.A. et al. (Eds), Vienna.
13. Fulland, M., Schöllmann, M., Richard H.A. (2001) In: *Advances in Fracture Research*, Ravi-Chandar, K. et al. (Eds), ICF10, Honolulu.
14. Kuhn, G., Kolk, K. (2003) In: *Proc. of the 15th Int. Conf. on Computer Methods in Mechanics*, CD, Burczynski, T. et al. (Eds), CMM2003, Gliwice, Poland.